ELSEVIER

Marine Geology 231 (2006) 51–67

MARINE GEOLOGY
INTERNATIONAL JOURNAL OF MARINE GEOLOGY, GEOCHEMISTRY AND GEOPHYSICS

www.elsevier.com/locate/margeo

Acoustic investigation of cold seeps offshore Georgia, eastern Black Sea

Ingo Klaucke [a,*], Heiko Sahling [b], Wilhelm Weinrebe [a], Valentina Blinova [c], Dietmar Bürk [a], Nona Lursmanashvili [d], Gerhard Bohrmann [b]

[a] *IFM-GEOMAR, Leibniz Institute of Marine Sciences, Wischhofstr. 1-3, 24148 Kiel, Germany*
[b] *Research Centre Ocean Margins, Bremen University, Postbox 330440, 28334 Bremen, Germany*
[c] *Department Geology and Geochemistry, Faculty of Geological Sciences, Moscow State University, Moscow, Russia*
[d] *Seismometrical Laboratory, Tbilissi State University, Tbilissi, Georgia*

Received 9 August 2005; received in revised form 26 May 2006; accepted 30 May 2006

Abstract

Several gas seeps and near-surface gas hydrate deposits have been identified in 850–900-m water depth on the continental slope offshore Batumi, Georgia (eastern Black Sea) using deep-towed high-resolution sidescan sonar data. The seeps are located on a ridge named Kobuleti Ridge separating two canyons: the Supsa canyon north of the ridge and the deeply incised central canyon south of it. The southern wall of this canyon shows signs for additional gas seeps. Gas seeps are shown by acoustic anomalies in the water column on raw sonar records and as high backscatter intensity areas on processed data.

The seeps on Kobuleti Ridge are characterised by carbonate deposits at the centre and a much wider area where finely disseminated gas hydrates are present. Fractures of a NW–SE direction are present at the seep sites and are probably related to the formation and decomposition of gas. Individual sites of gas emission apparently exert their influence for a circular area of up to 40 m in diameter. Gas geochemistry from gravity cores shows high gas content and a mixture of biogenic and thermogenic gases together with the presence of gas hydrates.

The seeps offshore Georgia are different from other known cold seeps in the Black Sea such as shallow water seeps of biogenic gas and deep water mud volcanoes. They are located in deep water within the zone of gas hydrate stability, lack significant relief and are characterised by active gas emission and the absence of mud volcanism.

Keywords: Black Sea; sidescan sonar; cold seep; gas hydrates; methane; Georgia

1. Introduction

The Black Sea is the Earth's largest anoxic basin with high methane concentrations of up to 11 μmol/L in the deeper water column amounting to a total inventory of 6×10^{12} mol of methane (Reeburgh et al., 1991). Major sinks of methane are the anaerobic oxidation of methane in water depths below and at the oxic/anoxic interface (99% of the total flux at 2.9×10^{11} mol/yr) followed by loss to the atmosphere (0.9% of the total at 4.1×10^{9} mol/yr). These rates are extremely high compared to the total inventory and result in residence times of methane in the Black Sea as low as 20 yr. Reeburgh et al. (1991) considered the decay of organic matter in areas comprised

* Corresponding author.
E-mail address: iklaucke@ifm-geomar.de (I. Klaucke).

0025-3227/$ - see front matter © 2006 Elsevier B.V. All rights reserved.
doi:10.1016/j.margeo.2006.05.011

between 100- and 1500-m water depth as the only source of methane in the Black Sea. Submarine methane sources from mud volcanoes or cold seeps were not considered in these budgets.

Since the work of Reeburgh et al. (1991) a large number of submarine methane sources have been identified in the Black Sea (Egorov et al., 2003). A couple of thousand methane seeps were found in only a small area of the NW Black Sea margin and their contribution to atmospheric methane concentrations are presently the focus of the EU-funded CRIMEA project (Naudts et al., 2006; http://www.crimea-info.org). Their influence on the methane budget of the anoxic basin is unknown. Schmale et al. (2005) estimated the methane flux to the atmosphere for this area and derived a sea-air methane flux similar to the estimates by Reeburgh et al. (1991).

Many submarine mud volcanoes have also been found in the Black Sea and studied in the framework of the UNESCO-IOC Training Through Research programme (Limonov et al., 1997; Bouriak and Akhmetjanov, 1998; Mazzini et al., 2004). A significant input of methane to the atmosphere from such sources has been postulated (Dimitrov, 2003). On the other hand, based on geochemical modelling, Aloisi et al. (2004) concluded that submarine mud volcanoes in the Black Sea contribute to only 0.03% of the total methane input. However, this estimate may not be reliable and could be off by several orders of magnitude, as these estimates are based on measurements from only one mud volcano that is known to show highly variable activity and may not be representative. In addition, the assumed number of mud volcanoes in the Black Sea might be incorrect and, finally, methane emissions from cold seeps without morphologic expression are not included in the estimates. Also, microbial methane consumption in the Black Sea waters exceeds methane production (Rusanov et al., 2005). This balance can only be equilibrated by additional methane input from deep marine sources such as mud volcanoes and other cold seeps along the continental slopes.

In order to determine the relevance of submarine methane seepages for the methane budget of the Black Sea, all types of seepages have to be considered. This includes shallow water seepages, submarine mud volcanoes and a new type of gas seeps in the deep water offshore Georgia that is first described in this paper. Such seeps have the extent of submarine mud volcanoes, but do not involve material transport from depth and do not have a morphological expression. Therefore, they are easily overlooked unless identified through sidescan sonar mapping. These are first results of the new German collaborative research project METRO (http://www.rcom-bremen.de/Page1908.html), which aims at understanding and quantifying the impact of deep water sources of methane on the geochemistry of Black Sea sediments and waters.

2. Geological setting and previous work

The study area offshore Georgia is located at the eastern margin of the eastern Black Sea basin (Finetti et al., 1988). The Black Sea basin is composed of two subbasins that are separated by two prominent ridges: the Andrusov Ridge and the Archangelsky Ridge (Fig. 1). The formation of the Black Sea basin is generally believed to result from back-arc spreading during the northward subduction of the Thetis plate and has undergone several phases of extension and compression since the Cretaceous (Zonenshain and Le Pichon, 1986; Nikishin et al., 2003). Both subbasins are subject to active deformation resulting from the ongoing northward movement of the Arabian plate and westward escape of the Anatolian block (Barka and Reilinger, 1997; Rangin et al., 2002). Deformation of the eastern subbasin is compressional and evident by active northward thrusting of the Pontides Fold Belt, southward thrusting of the Greater Caucasus Fold Belt and strike-slip motion along the North Anatolian fault (Barka and Reilinger, 1997).

Sedimentary thickness in both subbasins is enormous with Neogene–Quaternary deposits up to 12 km in thickness in the western subbasin. These deposits are generally highly reflective, well stratified and hardly faulted in seismic data although many diapiric structures are present in the northeastern part of the eastern subbasin and southeast of Crimea (Tugolesov et al., 1985). Many intervals of the Neogene succession are rich in organic matter, but the Late Oligocene–Miocene Maikopian Formation in particular represents good hydrocarbon potential.

Part of the most recent Quaternary deposits is also rich in organic matter. A common stratigraphic succession for the uppermost 10 m has been recognised to be present for most of the Black Sea basin (Ross and Degens, 1974; Degens and Stoffers, 1980; Limonov et al., 1994). This succession consists of olive-grey marine clays overlying sapropel layers with coccolith oozes. The sapropel layers gradually evolve from grey brackish-limnic clay deposits that contain progressively more turbidite layers in the deeper succession. A common feature of these brackish-limnic deposits is secondary pyrite formation due to the anaerobic oxidation of methane at sulphate–methane interface (Neretin et al., 2004).

The easternmost margin of the Black Sea offshore Georgia is characterised by the Greater Caucasus Thrust Belt in the North and the Adjara-Trialet Thrust Belt,

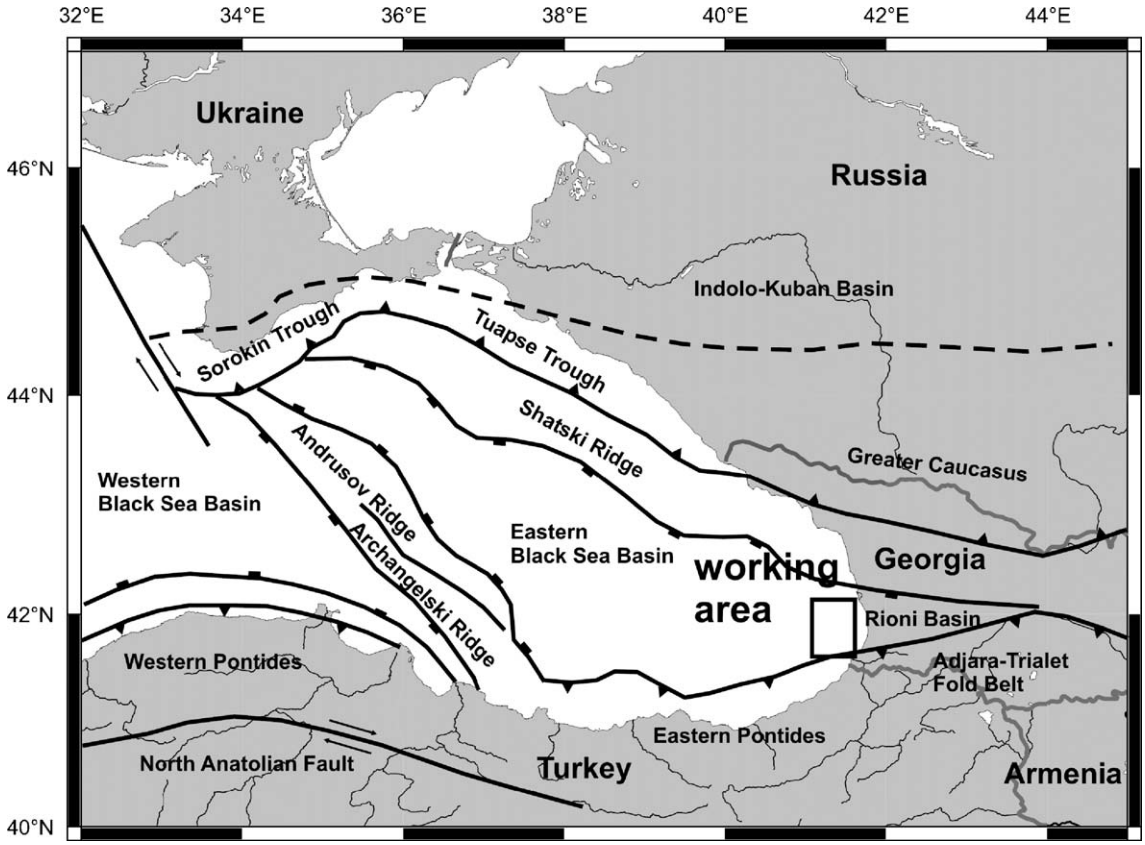

Fig. 1. Map of the eastern Black Sea basin and adjoining areas showing the study area and major tectonic units discussed in the text.

which is part of the eastern Pontides, in the South (Banks et al., 1997). Between the thrust belts two foreland basins developed in Georgia: the Kartli Basin extending into the Caspian Sea in the east and the Rioni Basin extending into the Black Sea in the west (Fig. 1). Sedimentation patterns for the two basins changed over time due to the uplift of the Greater Caucasus. Now most of the sediments are shed into the Rioni Basin for more than 1000-m-thick deposits of Plio-Quaternary sediments. Within the Rioni Basin, several E–W stretching anticline structures have been identified (Banks et al., 1997). Similar structures are also present in the eastern Black Sea and are frequently associated with acoustic anomalies in seismic records and gas emissions on the seafloor (Tugolesov et al., 1985; Egorov et al., 2003).

3. Database

Analysis and interpretation of fluid flow structures offshore Georgia are based on combined bathymetric, sidescan sonar and coring data obtained during *FS Poseidon* cruise P317/4 (16 October–4 November 2004) to the Black Sea (Sahling et al., 2004). Fluid escape structures with a distinct morphology and can be easily identified with bathymetric data while those structures lacking morphology appear as high backscatter patches on sidescan sonar records. Both geoacoustic datasets require ground-truthing and only an integrated approach allows a geologically meaningful interpretation of the data.

Bathymetric data have been obtained using a portable ELAC Bottomchart Mk II with 50 kHz transducers deployed in the moon pool of *FS Poseidon*. The opening angle of the total swath was set to 80° resulting in a swath width ranging from about 850 m in 500-m water depth to about 2500 m in 1500-m water depth. The system has a beam angle of 1.5 × 1.5° resulting in a footprint of 13 and 40 m, respectively. Data have been manually cleaned, processed and gridded using MB systems with a grid cell size of 50 m (Fig. 2).

Sidescan sonar data have been obtained with the digital, deep-towed DTS-1 system operated by IFM-GEOMAR. The DTS-1 is a modified EdgeTech dual-frequency chirp system working with 75 and 410 kHz

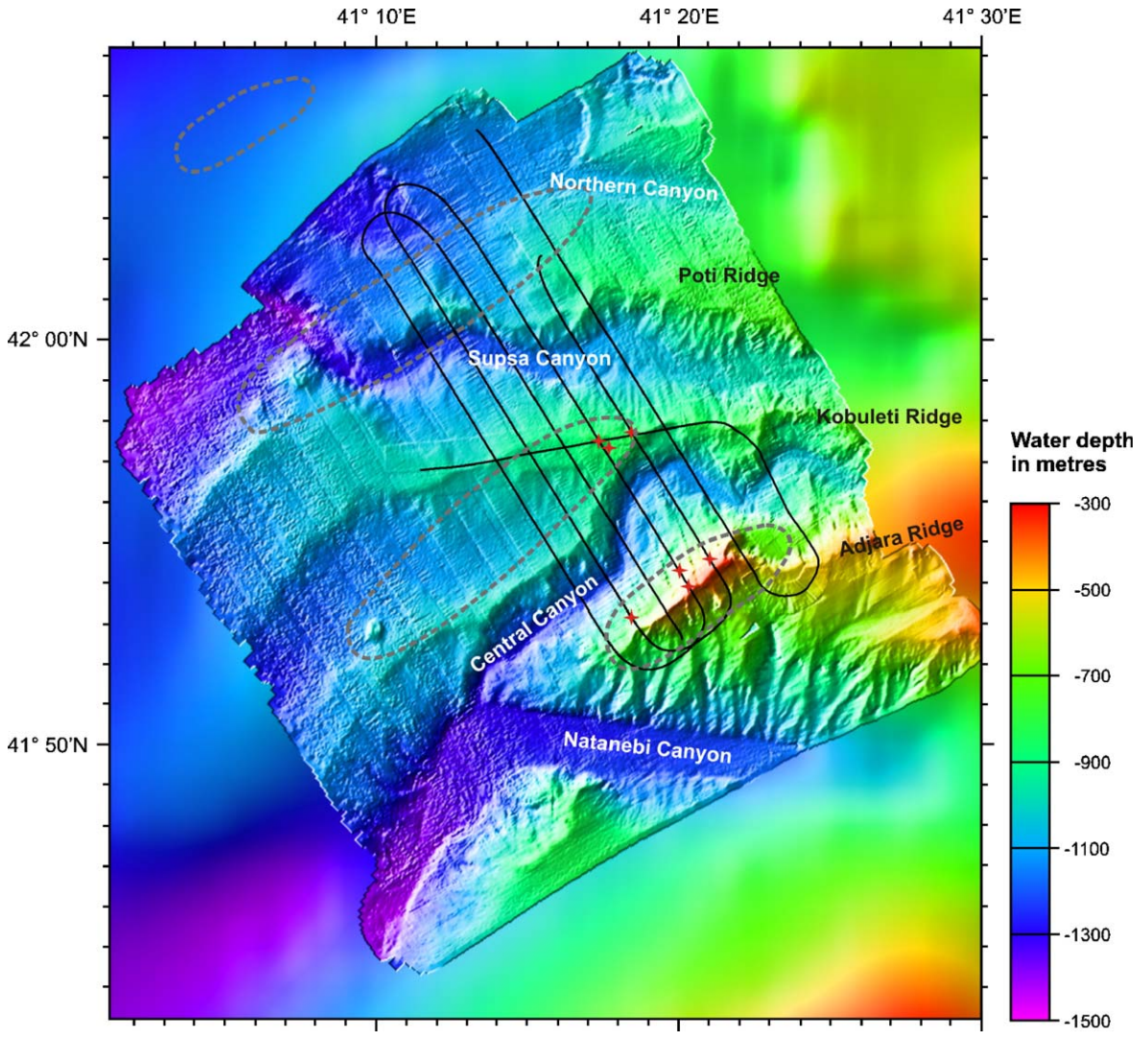

Fig. 2. Bathymetric map of the continental slope offshore Georgia (eastern Black Sea). The detailed central part is based on 50 kHz ELAC Bottomchart Mk-II multibeam data with a grid cell size of 50 m, while the rest shows data from the GEBCO 1-min grid. The red stars show the location of gas seeps offshore Georgia (Table 1) and the dotted lines indicate the extent of diapiric anticline structures at depth (Tugolesov et al., 1985).

centre frequencies for a maximum range of 750 and 150 m, respectively. The 75 kHz signal is a 14 ms long pulse of 7.5 kHz bandwidth providing an across-track resolution of 5.6 cm. The 410 kHz signal has a bandwidth of 40 kHz and 2.4 ms duration for an across-track-resolution of 1.8 cm. Towing speed averaged 2.5 knots and the data have been processed for a pixel size of 1.0 and 0.25 m, respectively, using the PRISM package from Southampton Oceanography Centre (Le Bas et al., 1995). The DTS-1 also includes a Chirp subbottom profiler operating with a 2–8 kHz and 20 ms pulse. Six parallel 75 kHz profiles have been collected covering a total of 185 km^2 (Fig. 3) together with one profile of 410 kHz sidescan sonar. Navigation of the towfish is based on the ship position and cable length using a layback method that integrates towing speed. This method gives good results except for turns although the degree of lateral deviation of the towfish can not be estimated. Data of the Chirp subbottom profiler have to be corrected for varying water depth of the towfish. During *FS Poseidon* cruise P317/4 data from a depth sensor mounted on the towfish were not available. Corrections to the raw profiler data have been made by adjusting the registered profile to a bathymetric profile

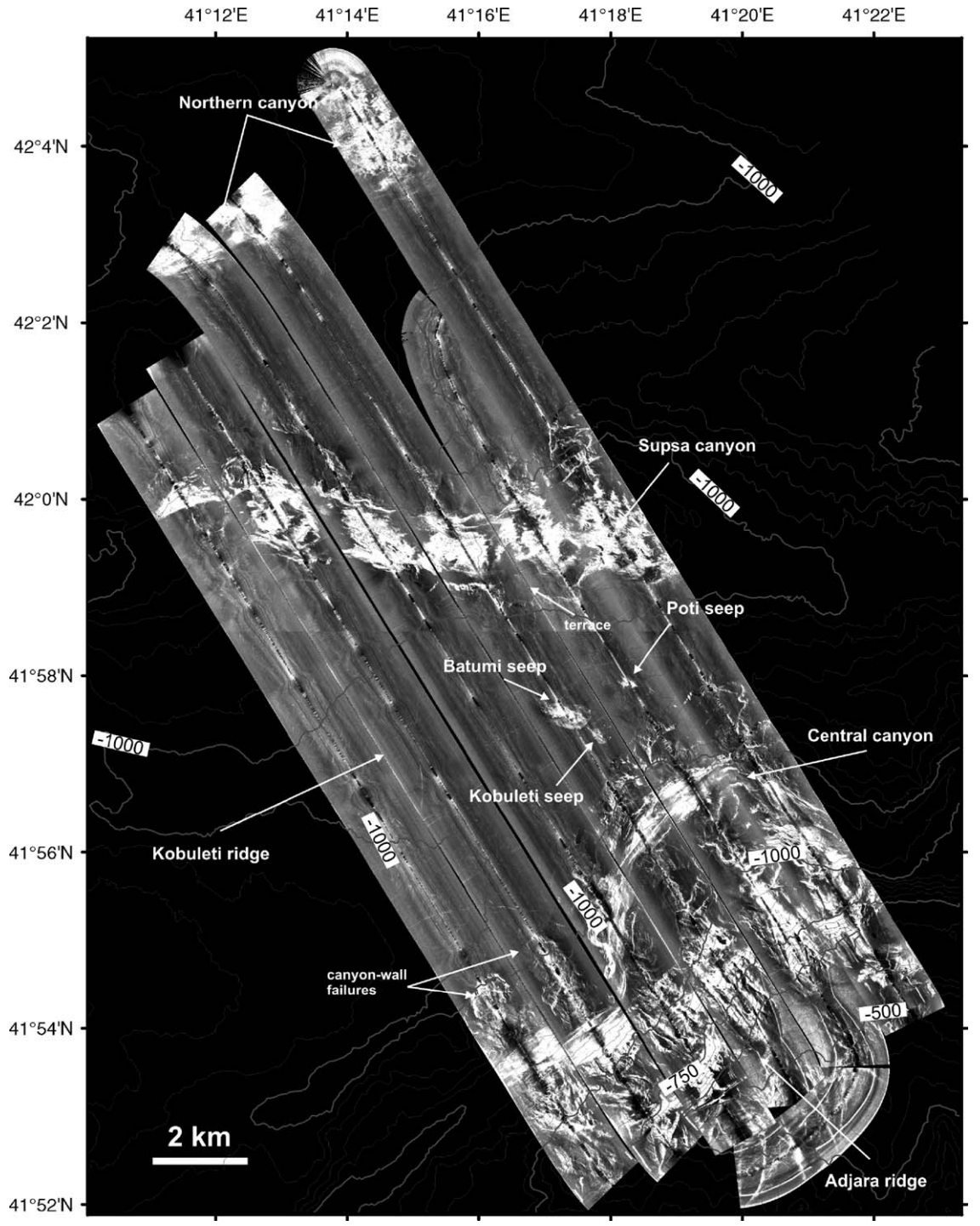

Fig. 3. Mosaic of 75 kHz DTS-1 sidescan sonar profiles showing the canyon and ridge canyon system on the middle continental slope offshore Georgia. Each swath is 1500 m wide and pixel size is 1 m. The sidescan sonar data are shown in normal polarity, i.e. high backscatter intensity is white. Contour interval is 50 m.

obtained from the multibeam grid. Features with vertical displacement less than the resolution of the grid are consequently no longer resolved.

Ground-truthing of the geoacoustic data was possible through towed video observations and five short gravity cores. Two cores used a plastic bag instead of a liner for

immediate inspection onboard and three cores had a plastic liner for subsequent analysis in the lab. The non-liner cores have been sampled for methane analysis using a standard headspace method.

4. Fluid venting

The continental slope offshore Georgia is dissected by several canyons that are separated by sharp-crested ridges.

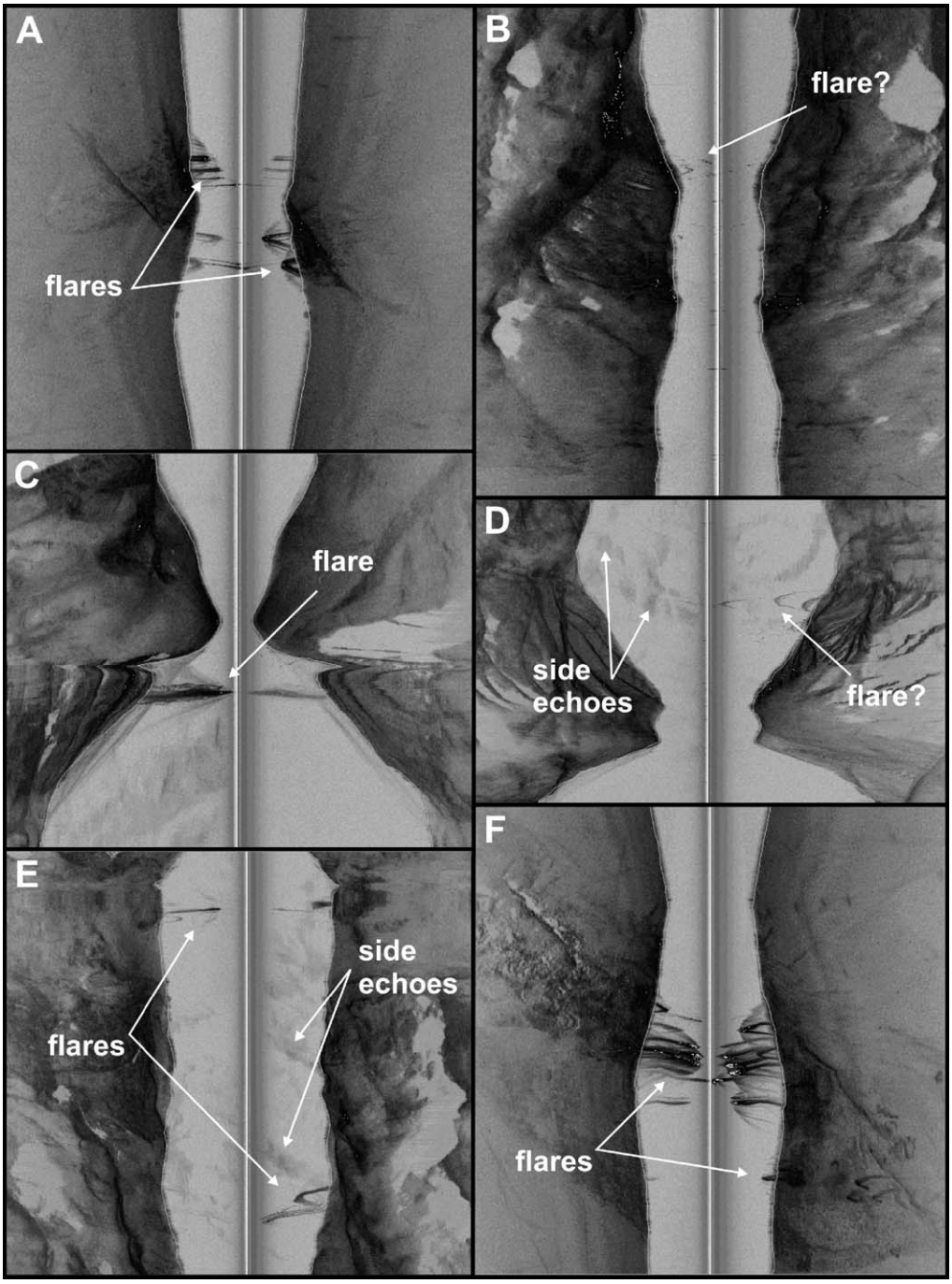

Fig. 4. Unprocessed sidescan sonar records showing backscatter anomalies within the water column at various locations offshore Georgia. (A) Poti seep. (B and D) Probable flares near ridge crest of the northern flank of Adjara ridge. (C and E) Flares along the northern flank of Adjara Ridge and F. Batumi seep. The sidescan sonar data are shown in inverse polarity, i.e. high backscatter intensity is dark.

From north to south, these are: Northern canyon, Poti Ridge, Supsa canyon, Kobuleti Ridge, Central canyon, Adjara Ridge and Natanebi canyon (Fig. 2). Indications for gas and fluid seepage are present in two areas: on Kobuleti Ridge and the northern flank of Adjara Ridge, which is also the southern flank of Central canyon. Fluid seepage on the canyon flanks is only observed as acoustic anomalies in the water column (Fig. 4B–E), while the

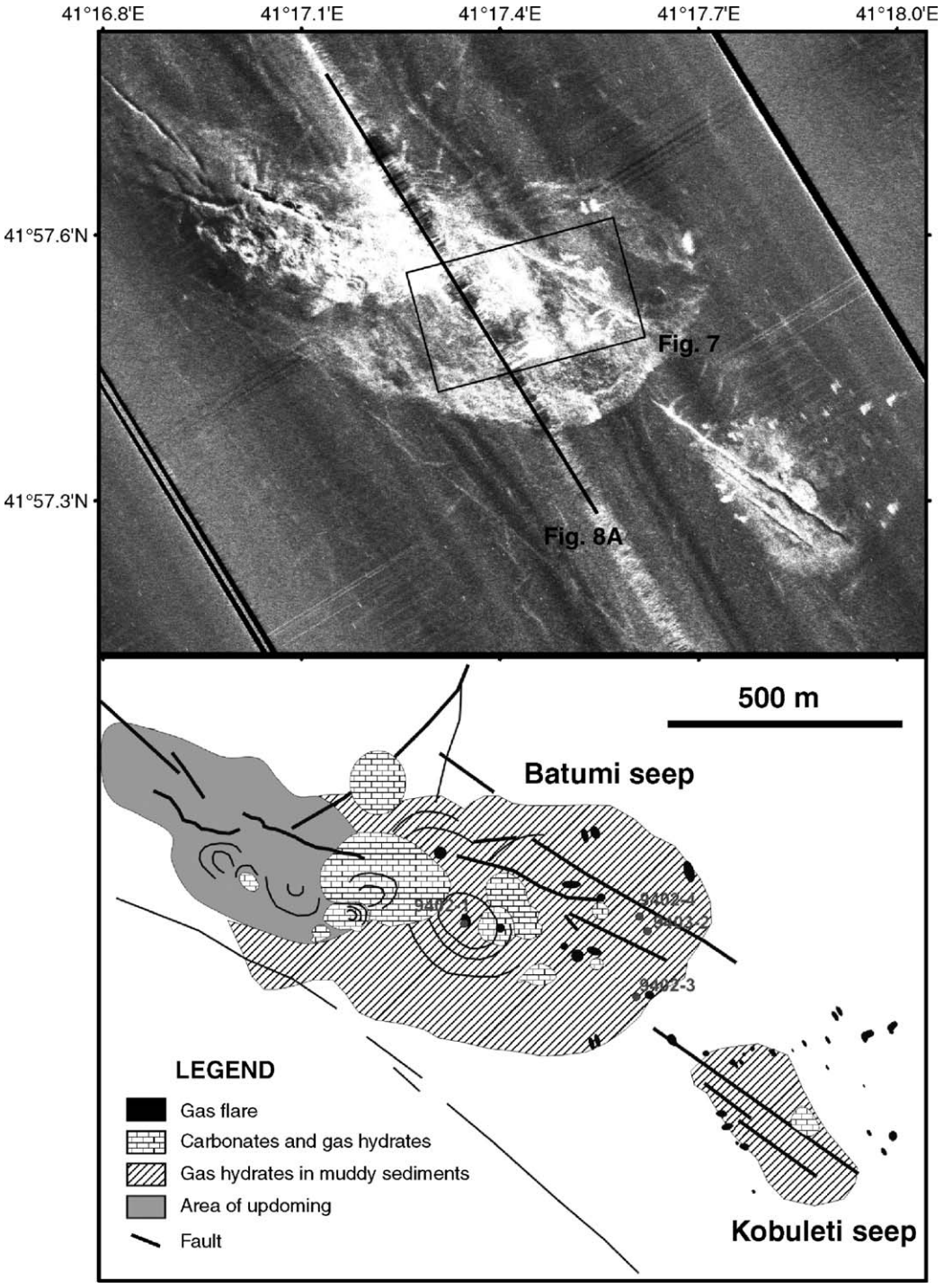

Fig. 5. 75 kHz DTS-1 sidescan sonar mosaic and interpretation of Batumi and Kobuleti seeps. High backscatter intensity is shown in light tones and low backscatter intensity or shadows in dark tones.

Table 1
Locations of gas seeps offshore Georgia

No.	Latitude	Longitude	Water depth	Remarks
1	41°57.50N	41°17.33E	860 m	Batumi seep identified by anomalies in the water column and high backscatter intensity on sidescan sonar records (Fig. 4F)
2	41°57.30N	41°17.82E	860 m	Kobuleti seep identified by high backscatter intensity on sidescan sonar records
3	41°57.90N	41°18.24E	890 m	Poti seep identified by anomalies in the water column and high backscatter intensity on sidescan sonar records (Fig. 4A)
4	41°52.91N	41°18.65E	600 m	Acoustic anomaly in the water column on the upper canyon wall (Fig. 4C)
5	41°54.78N	41°19.62E		Acoustic anomaly in the water column on the middle canyon wall (Fig. 4E)
6	41°54.61N	41°21.00E		Acoustic anomaly in the water column on the upper canyon wall (Fig. 4E)
7	41°54.50N	41°19.85		Small acoustic anomaly in the water column on the upper canyon wall (Fig. 4D)

seepage areas on the crest of Kobuleti Ridge are imaged by both acoustic anomalies in the water column (Figs 4A and F) and high backscatter intensities on the seafloor (Fig. 3). Unprocessed sidescan sonar data in a typical waterfall display show a central area of no or extremely low backscatter intensity corresponding to returns from within the water column (Fig. 4). The contact between the water column and the seafloor is marked by a strong and sudden increase in backscatter intensity. High backscatter anomalies from within the water column as shown in Fig. 4 can be the result of gas bubbles or fish. The latter can be excluded in the Black Sea below the oxic/anoxic interface.

4.1. Characteristics of seep locations

Kobuleti Ridge is the site of three individual seep areas that are characterised by elevated backscatter intensity on sidescan sonar mosaics (Fig. 3) and that show acoustic anomalies in the water column (Fig. 4A and F). The largest of these seeps centred on 41°57.5N and 41°17.33E has been named Batumi seep and covers a total area of 0.5 km^2 (Fig. 5, Table 1). A smaller seep area just to the southeast of Batumi seep is called Kobuleti seep and extends over 0.07 km^2. The third seep area further up slope has been named Poti seep and covers only 0.05 km^2 (Fig. 6). There is active gas emission in the form of gas bubbles from these sites as evidenced by gas flares in the water column of unprocessed 75 kHz sidescan sonar records (Klaucke et al., 2005). In addition, several high backscatter patches on processed sidescan sonar records have been interpreted as gas flares. Some of the high backscatter patches have a curved shape and are clearly related to gas flares. Other high backscatter patches do not have a distinctive signature, but are still interpreted as gas flares, because most of them occur isolated within a low backscatter surrounding. It cannot be excluded, however, that the high backscatter is the result of different lithology such as carbonate crusts instead of gas flares.

4.1.1. Batumi seep

The largest seep of the study area appears to be formed around three N120 trending fractures. Some of the gas flares coincide with the trace of these fractures (Fig. 5), but many other gas flares identified by high backscatter intensity on sidescan sonar records are unrelated to fractures. The most intense fracturing is present in the west of the seep area: an area that is also characterised by moderate updoming of the seafloor. There are at least four concentric areas of high backscatter intensity on the southern flanks of this dome. The centre of these rings shows low backscatter intensity, which points to a possible depression.

The central part of the seep area is characterised by very high backscatter intensity and coincides with gas flares in the water column. This part of the seep area does not show strong relief although subbottom profiler records show a rough surface with no subbottom reflections and poor signal penetration. Several concentric structures are apparent and are better imaged on 410 kHz sidescan sonar records (Fig. 7). They are up to 40 m in diameter and composed of several rings of alternating high and low backscatter intensity. The differences in backscatter intensity are probably related to small-scale relief of the seafloor that becomes apparent due to the low towing altitude of generally less than 20 m. The ring structures are highly imbricate in the central part of the seep indicating many closely spaced or overlapping gas seeps. The central seep area is surrounded by a halo of non-uniform, patchy medium backscatter intensity (Fig. 5). The contact between this medium backscatter facies and the surrounding background sediments is sharp.

4.1.2. Kobuleti seep

Kobuleti seep is located 250 m southeast of Batumi seep. It is much smaller than its neighbour (0.07 km^2 compared to 0.5 km^2) and characterised by three parallel fractures of which the longest (530 m long) shows an inversion of throw direction (Fig. 5). Several gas flares

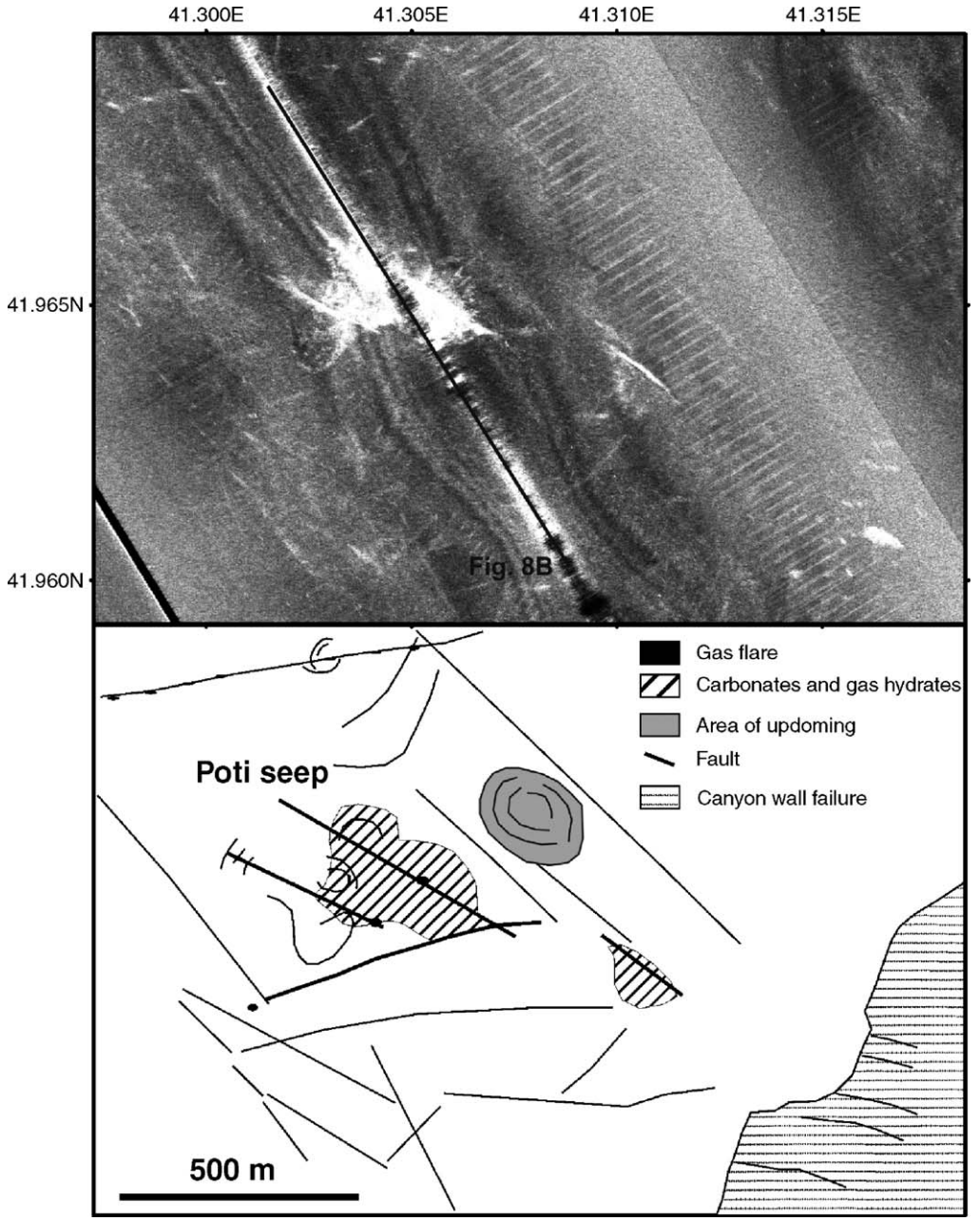

Fig. 6. 75 kHz DTS-1 sidescan sonar mosaic and interpretation of Poti seep. High backscatter intensity is shown in light tones and low backscatter intensity or shadows in dark tones.

(identified as high backscatter patches, some of which have curved tails) originate directly from the main fracture. However, other high backscatter patches are present. Some of them are aligned along a west–east direction and are more or less equally spaced, but no fracture is visible along this same direction (Fig. 5). Similar to Batumi seep, there is one area with high backscatter intensity, but most of the seep area shows medium backscatter intensity. One remarkable feature is the main fracture that extends beyond the area of increased backscatter intensity and that shows gas flares outside of the seep area.

4.1.3. Poti seep

The smallest seep area (0.05 km^2) on the same ridge is located several hundreds of metres further up slope and also associated with three N120 fractures (Fig. 6). The

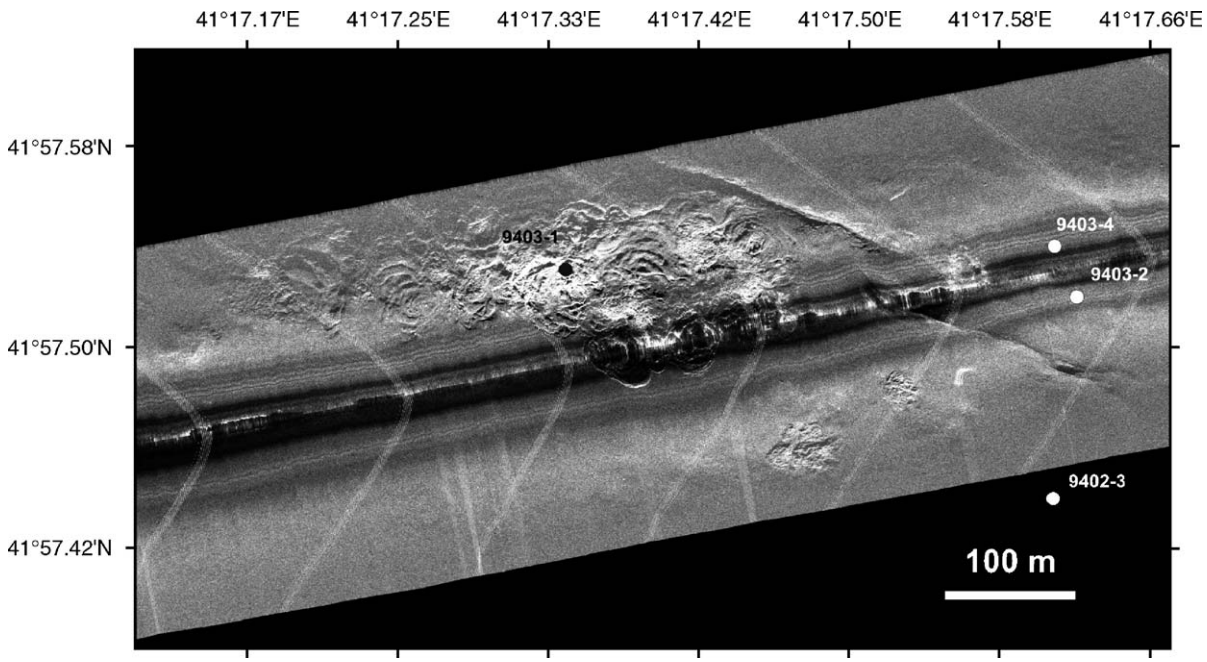

Fig. 7. 410 kHz DTS-1 sidescan sonar profile across Batumi seep showing two fractures in the east and individual seeps with concentric rings. The sidescan sonar image here is dominated by small-scale relief, due to very high sonar frequencies and low towing altitude (25 m). High backscatter is shown in light tones.

longest of these fractures reaches 450 m in length while the two other fractures are only 250 m long. They seem to delimit an area of very high backscatter intensity coinciding with many acoustic anomalies in the water column (Fig. 4A). Several spots of very high backscatter intensity are also visible on processed sidescan sonar records and probably correspond to the image of gas flares on the seafloor (Fig. 6). On 2–8 kHz Chirp subbottom profiler records, this central area is not penetrated by the signal and presents a typical signature for gas charged sediments (Fig. 8). There is limited relief of the structure of less than 15 m. A halo of medium backscatter intensity around the central seep as for Batumi and Kobuleti seeps is not observed. Just to the southeast of Poti seep another short (200 m long) fracture exists with no indication of gas flares. Elevated backscatter intensity on the seafloor, however, suggests some local updoming of the seafloor that is probably also related to fluid seepage.

4.1.4. Canyon wall seeps

Gas flares along the northern, steep slope of Adjara Ridge have been observed on raw sidescan sonar data at five locations. These flares are much smaller than the flares on Kobuleti Ridge and generally only show single anomalies in the water column instead of several anomalies for the seeps on Kobuleti Ridge. Unfortunately, due to strong relief, it is not possible to relate the seeps to a specific backscatter facies on the seafloor. Only one location suggests elevated backscatter intensity associated with the flare (Fig. 4E). The flares are mostly concentrated near the summit of the ridge, but one flare is seen at mid height of the ridge flank (Fig. 4E, Table 1). The northern flank of Adjara Ridge forms by incision of the central canyon, which exposes slope strata that may form conduits for fluids seeping out at distinct high permeability layers.

4.1.5. Other possible seep locations

The 75 kHz sidescan sonar data also show several other lineations of elevated backscatter intensity whose origin remains unclear. Some of these lineations show a criss-cross pattern similar to that described elsewhere in the Black Sea (Limonov et al., 1997). These authors reported a correlation of the criss-crossing lines with accumulations of shells. Offshore Georgia some of the lines seem to be correlated with small backscatter anomalies at the seafloor and in the water column of raw 75 kHz sidescan sonar data (Fig. 9). This suggests that the lineations on the sidescan sonar mosaics might be due to elevated gas concentrations in the uppermost sediments and the water column anomalies are very small gas flares of up to 10-m height. This, however, must remain speculation without further investigation.

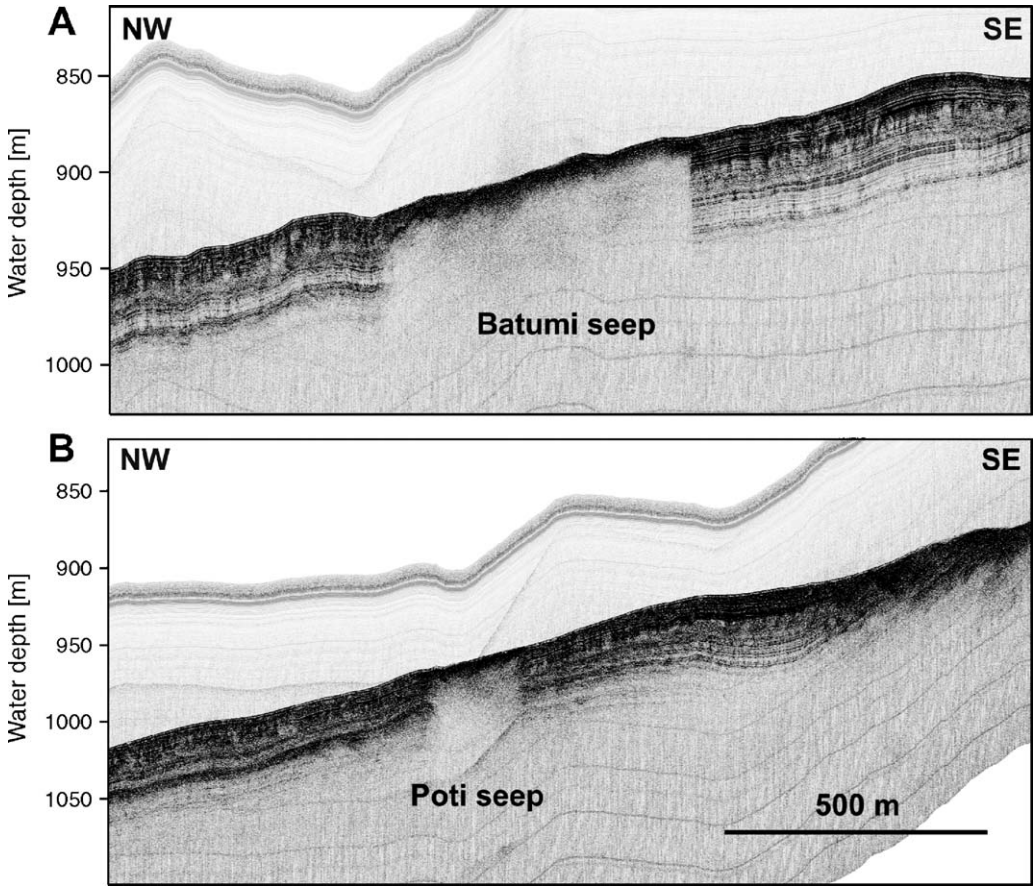

Fig. 8. 2–8 kHz Chirp profiles across Batumi (A) and Poti (B) seeps. Profile locations are shown in Figs. 5 and 6. The reflection located 60–120 m above the seafloor corresponds to the water depth of the towfish.

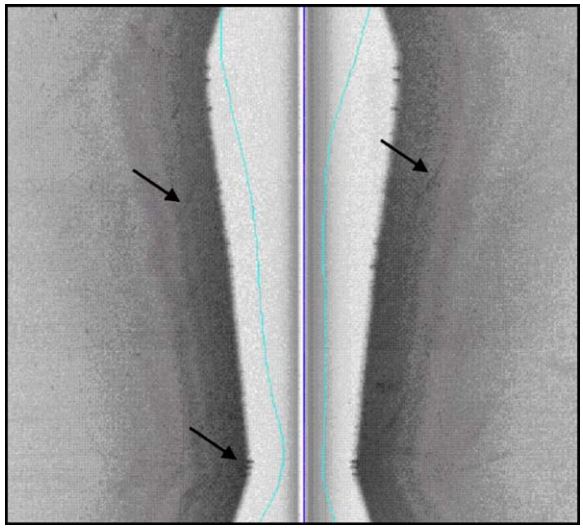

Fig. 9. Examples of unprocessed 75 kHz sidescan sonar data of backscatter anomalies that could be related to gas emissions. Arrows indicate possible small gas flares correlating with lineations on the sonar record.

Table 2
Locations of sediment cores from offshore Georgia

Core [GeoB]	Latitude	Longitude	Water depth (m)	Core length (cm)	Acoustic facies
9402-3	41°57.44E	41°17.61N	860	245	Low backscatter background
9403-1	41°57.53E	41°17.34N	859	184	High backscatter at the centre of Batumi seep
9403-2	41°57.52E	41°17.62N	860	205	Medium backscatter at the margin of Batumi seep
9403-3	41°56.85E	41°17.29N	913	545	Low backscatter background
9403-4	41°57.54E	41°17.61N	861	50	Medium backscatter at the margin of Batumi seep

Finally, the high-resolution bathymetry obtained offshore Georgia shows two almost circular structures in the prolongation of Kobuleti ridge (Fig. 2). These structures are about 1500 m in diameters and reach up to 100 m of relief height over the surrounding seafloor. The nature and origin of these structures remain unclear, but they morphologically resemble submarine mud volcanoes in other parts of the Black Sea (Limonov et al., 1997; Bohrmann et al., 2003).

4.2. Ground-truthing

Ground-truthing of the sidescan sonar mosaic was possible through 4 cores taken at three locations showing different backscatter facies of the sidescan sonar mosaic (Table 2) and through two video tracks.

4.2.1. Core GeoB-9403-1

This core was taken in an area of very high backscatter intensity at the centre of Batumi seep on the Kobuleti Ridge (Fig. 5). It shows two intervals composed of broken carbonate pieces at the top of the core (15 cm thick) and in 37-cm subbottom depth (28 cm thick, Fig. 8). The carbonate pieces are rounded and up to a few centimetres in diameter. Some are olive grey in colour, others show signs of whitish coccoliths and some have brownish stains due to iron-sulphides. These two units of broken carbonate are separated by a 22-cm-thick interval of olive-grey mud with whitish mm-thick layers of coccolith ooze. The second carbonate interval directly overlies grey clay deposits that were completely liquefied by gas hydrate decomposition.

4.2.2. Cores GeoB-9402-3 and GeoB-9403-2

Cores GeoB-9402-3 and GeoB-9403-2 were taken from an area of intermediate backscatter intensity at the eastern margin of Batumi seep (Fig. 5). Both cores show a very similar stratigraphic succession of light olive grey mud with many millimetre-thick coccolith ooze layers (Fig. 10). These deposits also contain several thin turbidites of up to 2 cm in thickness. Some of the coccolith ooze layers are already cemented and form millimetre-thick carbonate crusts. Below 60-cm subbottom depth, the core shows strong signs of degassing (foamy structure) although some intervals preserved the marine clay and coccolith ooze alternations. Deeper in the core the coccolith layers gradually decrease and the internal structure of the core was completely destroyed probably due to gas hydrate decomposition. There was strong degassing and a smell of hydrogen sulphide during recovery of the core. Below the interval containing gas hydrate a 65-cm-thick unit of olive-grey clay containing in the lower part, many bands of hydrotroilite exist. The upper boundary of the hydrotroilite is oblique to the stratification. The base of core GeoB-9403-2 below 165-cm subbottom depth shows again light olive-grey clay deposits that are very watery but preserved faint lamination and few whitish coccolith laminae.

4.2.3. Core GeoB-9403-3

This core was taken in background deposits of low backscatter intensity on Kobuleti Ridge in the vicinity of Batumi seep. The core shows the typical succession of Late Quaternary Black Sea sediments (Limonov et al., 1994). The top of this core shows a 30 cm thick interval of very fine laminations of olive-grey marine clay. This interval overlies very finely laminated deposits of whitish coccolith ooze alternating with olive-grey clays. Deeper in the core these deposits give way to alternations of dark and light grey clays, some of which are laminated while others are heavily bioturbated. At 253-cm subbottom depth, a 53-cm-thick unit of black clay containing much hydrotroilite has been found. The lower section of this core below 306-cm subbottom depth is composed of laminated alternating olive-grey and beige silty clays and 1–3-mm-thick silt layers. This probably represents alternating turbidites and hemipelagic intervals.

4.2.4. Video observations

Two lines with a towed video camera have been obtained over flares at Batumi seep. One line was following the sidescan sonar track and one crosses the

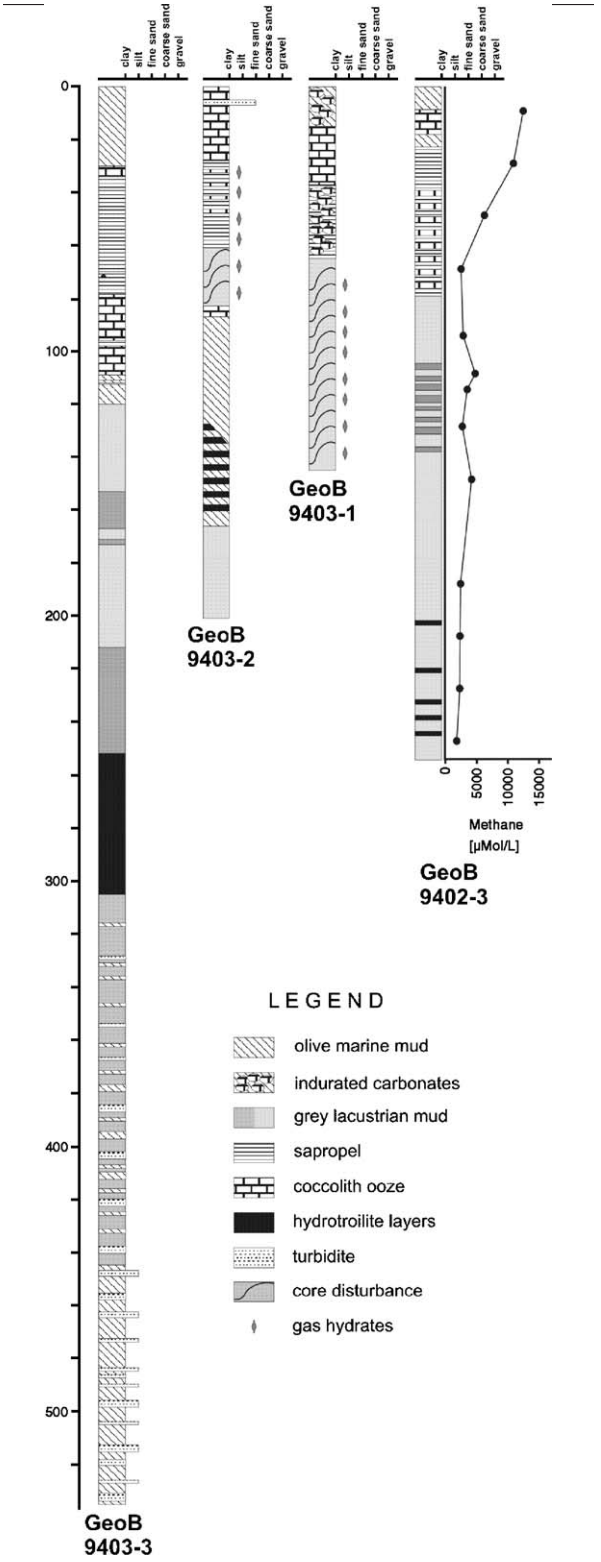

Fig. 10. Logs of gravity cores and methane profile for sediment cores taken. For core location refer to Figs. 5, 6 and 7. Core GeoB 9403-1 was taken from the high backscatter area, cores GeoB 9403-2 from the intermediate backscatter area, and cores GeoB 9402-3 and 9403-1 from low backscatter background locations.

southern margin of the seep. The video observation shows changing sediment colours with a small area of whitish seafloor at the southern margin of the seep and very dark sediments at the centre. The whitish seafloor might represent bacterial mats and the dark sediments are probably rich in hydrogen sulphide, but evidence from the video runs is not conclusive. Seafloor disturbances at the traces of the fractures are also visible, but there were no indications of carbonate outcrops or mudflows.

4.3. Gas geochemistry

Gases from two sediment cores were collected and are mostly composed of methane with concentrations reaching 13,000 µmol/L at the seafloor and an average of 2500 µmol/L below 75-cm subbottom depth. Small additions of ethane (up to 3.5 µmol/L), propane (up to 8.0 µmol/L) and butane (up to 19 µmol/L in total) are present. Stable carbon isotope $\delta^{13}C$ values of methane are around −53‰ PDB and reach values of −57.4‰ near the surface. In addition to the gases small, thin plates of gas hydrate have been collected at subsurface depths ranging from 145 to 200 cm. Gas from the hydrates (pure methane) has a $\delta^{13}C$ value of −53.3‰ PDB, which is similar to the free gas sampled from the cores.

5. Discussion

Gas seeps in the Black Sea in general and offshore Georgia are known since ancient times, but have been studied more systematically only recently (Egorov et al., 2003). Two main types of cold seeps have been observed: gas emissions in shallow water down to about 725 m (Michaelis et al., 2002; Egorov et al., 2003; Naudts et al., 2006) and submarine mud volcanoes (Limonov et al., 1997; Bouriak and Akhmetjanov, 1998) in water depth ranging between 1000 and 2000 m. The cold seeps offshore Georgia are different from these two types because they occur within the zone of gas hydrate stability, whose upper limit is around 725-m water depth in the eastern Black Sea (after Sloan, 1990 and based on 9 °C bottom water temperature). In addition, the seeps offshore Georgia do not seem to involve mud flow from depth as it occurs in mud volcanoes.

5.1. Sidescan sonar imaging of cold seeps

Gas seeps within the limit of gas hydrate stability have been found in other areas such as Hydrate Ridge (Suess et al., 1999), the Texas–Louisiana Slope (Leifer and MacDonald, 2003), offshore Angola (Charlou et al., 2004) or the Sea of Okhostsk (Shoji et al., 2005). In all these areas, gas seeps without a rough morphological relief have been reported. There are, however, some differences between these sites and the seeps offshore Georgia.

Firstly, the number of individual gas flares appears to be much higher offshore Georgia than in the other areas. This might be due to the imaging technique that has been used. At Hydrate Ridge, the Texas–Louisiana slope and the Sea of Okhotsk gas emission are imaged either through echosounder profiling or visual observation (MacDonald et al., 2000; Torres et al., 2002; Heeschen et al., 2003; Sassen et al., 2004; Shoji et al., 2005). Observations of gas flares on unprocessed sidescan sonar data are not reported, probably because data from the water column are not always available.

Secondly, the internal zoning of the seeps with areas of high and intermediate backscatter intensity is not known elsewhere. Most examples of sidescan sonar data from cold seeps show uniform high backscatter intensity (e.g. Johnson et al., 2003; Sager et al., 2004; Shoji et al., 2005) or the effect of small-scale relief (Luff et al., 2005). This difference in backscatter intensity could be the results of different sonar frequencies as the latter influences the across-track resolution and the signal penetration. However, sidescan sonar data of Johnson et al. (2003), Shoji et al. (2005) and this study have been processed to a final pixel size of 1 m and should consequently be comparable. One explanation for the zoning offshore Georgia might be differential burial underneath hemipelagic sediments as we go away from the centre of the seep. Such differences would be more easily detected with high-frequency sidescan sonar system whose signal is more strongly attenuated and whose signal penetration is lower than for low-frequency sonar systems (Stoll, 1986). Clearly, the ring-like structures seen on very-high-frequency sonar (Fig. 6) support this idea. On the other hand, increasing burial beneath hemipelagic sediments can not explain the sharp outer boundary of the seep nor the differences in lithology of the recovered sediments. In the absence of relief, differences in backscatter intensity must correspond to different lithologies. In the case of cold seeps offshore Georgia, the different backscatter intensities most likely reflect the extent of carbonate crusts and the concentration of gas hydrate in the uppermost sediments.

5.2. Processes of gas seepage offshore Georgia

Cold seeps in the Black Sea are a well known phenomenon. A great number of gas seeps have been observed in shallow water depth of less than 725 m, i.e. above the zone of hydrate stability (Egorov et al., 2003; Naudts et al., 2006). In addition, many mud volcanoes are known from both the Black Sea basin (Limonov et al., 1997) and adjacent land areas (Albov, 1971). The cold seeps offshore Batumi are different from these types, because they are located well within the zone of stability of gas hydrates. At the same time, they show the presence of gas plumes above the seep site, but lack the characteristics of submarine mud volcanoes. Signs of recent mud flows are absent on both the sidescan sonar and the subbottom profiler records (Figs. 5, 6 and 8). In addition, even sediment cores from the centre of the seeps (Fig. 10) did not retrieve mud breccia deposits of the Maikopian Formation as elsewhere in the Black Sea (Ivanov et al., 1996), but rather show a typical Black Sea succession as defined by Ross and Degens (1974) and Limonov et al. (1994).

The co-existence of free gas bubbles and gas hydrates within the zone of gas hydrate stability is possible in areas where elevated heat flow and/or the outflow high saline water from greater depth shift the hydrate stability field down (Bohrmann et al., 2003). Heat and salt inhibition of gas hydrate formation is also known from other areas like the Gulf of Mexico (Ruppel et al., 2005). The temperature and salinity of the fluids seeping out at the seafloor offshore Georgia is unknown, but an elevated heat flow at these locations could destabilise hydrates and form free gas bubbles. Another possibility is the inhibition of hydrate formation because of very high gas flux and insufficient availability of fresh water at depth or the presence of local high salinity zones as suggested by Tréhu et al. (2004) and Milkov et al. (2004), respectively. Finally, the difference between the composition of the gas hydrates and the free gas within the sediments could suggest that only methane gas is incorporated into the gas hydrates and that higher hydrocarbon gases remain in a gaseous state. However, with only one sample of gas hydrate analysed, this explanation must remain highly speculative and has to be elucidated further in subsequent studies. Higher hydrocarbons also point to a deep source of part of the gas and might indicate the presence of hydrocarbon reservoirs at depth.

5.2. Factors controlling seep distribution

There are several potential petroleum source rocks in western Georgia, but their extension offshore is not known (Robinson et al., 1997). For most of the Black Sea,

the Late Oligocene–Miocene Maikop Formation is the probable source for most of the mud volcanoes in the Black Sea area (Ivanov et al., 1996). In the eastern Black Sea, the Maikop Formation has been deformed into a number of E–W trending diapiric ridges (Tugolesov et al., 1985), probably due to tectonic loading by the Greater Causacus and the Achara-Trialet Thrust Belt (Banks et al., 1997). These ridges also appear to guide slope canyon orientation on the lower continental slope and rise (Fig. 2). Kobuleti Ridge is located above one of these structures. Diapirism always results in fracturing of the overlying deposits and provides the pathways for fluids expelled from deeper structures (Krastel et al., 2003). The small fractures observed on sidescan sonar records may well be part of the surface expression of these deep faults. However, the lateral extent of these fractures is much too small to account for deep-reaching faults related to diapirism at depth. Also, 75 kHz sidescan sonar only images very recent fractures and the fractures seen on the sidescan sonar mosaic (Figs. 5 and 7) are probably related to local deformation associated with the formation and dissociation of gas hydrates.

6. Conclusions

Three seep areas covering 0.5 km^2, 0.07 km^2 and 0.05 km^2 on Kobuleti Ridge have been mapped with high-resolution sidescan sonar in 850–900-m water depth offshore Georgia. The seeps are presently active methane gas emitters and characterised by gas flares in the water column and high backscatter anomalies on sidescan sonar records. The high backscatter correlates with carbonate precipitates probably resulting from anaerobic methane oxidation and near-surface gas hydrates on the seafloor. Individual gas seeps produce concentric rings of alternating high and low backscatter intensity and seem to extend their influence for up to 40 m around the gas seep.

Fluids escaping from the seeps point towards mixed thermogenic and biogenic gases, which suggests a deep component in the source of the fluid. There are, however, no signs for material transport from depth and mud extrusion can be excluded as a mechanism for the formation of these seeps. We propose the ascent of thermogenic gas from depth with subsequent admixing of biogenic methane as a source for the fluid. The actual driving mechanism for fluid flow must be related to the northward thrusting of the Adjara-Trialet Fold Belt and the tectonic overburden and diapirism resulting from it.

Estimates about the methane budget in the Black Sea can not be complete without including submarine sources. Whether their contribution is considered significant strongly depends on the number of methane seeps that are estimated. Data presented in this paper suggest that many sources are easily overlooked, because they do not have a morphological expression. As a consequence, extrapolations on the methane release from submarine cold seeps are probably underestimated.

Acknowledgements

Captain Schneider, his crew and the participating scientists of *FS Poseidon* cruise P317/4 are thanked for their invaluable help at sea in collecting the data. Tanja Fromm edited the bathymetric data. This is contribution GEOTECH-225 of the R&D-programme GEOTECHNOLOGIEN funded by the German Ministry of Education and Research (BMBF) and the German Research Foundation (DFG), project METRO (grant03G0604A).

References

Albov, S.V., 1971. The Kerch-Taman hydrogeochemical and mud volcano region. Trans. (Doklady) USSR Acad. Sci. 197, 237–239.

Aloisi, G., Drews, M., Wallmann, K., Bohrmann, G., 2004. Fluid expulsion from the Dvurechenskii mud volcano (Black Sea): Part I. Fluid sources and relevance to Li, B, Sr, I and dissolved nitrogen cycles. Earth Planet. Sci. Lett. 225, 347–363.

Banks, C.J, Robinson, A.G., Williams, M.P., 1997. Structure and regional tectonic of the Achara-Trialet Fold Belt and the adjacent Rioni and Kartli Foreland Basins, Republic of Georgia. In: Robinson, A.G. (Ed.), Regional and Petroleum Geology of the Black Sea and Surrounding Region. AAPG Memoir, vol. 68. AAPG, Tulsa, pp. 331–345.

Barka, A.A., Reilinger, R.E., 1997. Active tectonics of the eastern Mediterranean region: derived from GPS, neotectonic and seismicity data. Ann. Geofis. XL (3), 587–610.

Bohrmann, G., Ivanov, M., Foucher, J.P., Spiess, V., Bialas, J., Greinert, J., Weinrebe, W., Abegg, F., Aloisi, G., Artemov, Y., Blinova, V., Drews, M., Heidersdorf, F., Krabbenhoft, F., Klaucke, I., Krastel, S., Leder, T., Polikarpov, G.G., Saburova, M., Schmale, O., Seifert, R., Volkonskaia, A., Zillmer, M., 2003. Mud volcanoes and gas hydrates in the Black Sea: new data from Dvurechenskii and Odessa mud volcanoes. Geo-Mar. Lett. 23, 239–249.

Bouriak, S.V., Akhmetjanov, A.M., 1998. Origins of gas hydrate accumulation on the continental slope of the Crimea from geophysical studies. In: Henriet, J.-P., Mienert, J. (Eds.), Gas Hydrates: Relevance to World Margin Stability and Climatic Change. Geological Society Special Publication, pp. 215–222.

Charlou, J.L., Donval, J.-P., Fouquet, Y., Ondreas, H., Knoery, J., Cochonat, P., Levache, D., Poirier, Y., Jean-Baptiste, P., Fourre, E., Chazallon, B., ZAIROV Leg-2 Scientific Party, 2004. Physical and chemical characterization of gas hydrates and associated methane plumes in the Congo-Angola Basin. Chem. Geol. 205, 405–425.

Degens, E.T., Stoffers, P., 1980. Environmental events recorded in Quaternary sediments of the Black Sea. J. Geol. Soc. Lond. 137, 131–138.

Dimitrov, L., 2003. Mud volcanoes—a significant source of atmospheric methane. Geo-Mar. Lett. 23, 155–161.

Egorov, V.N., Polikarpov, G.G., Gulin, S.B., Artemov, Yu.G., Stokozov, N.A., Kostova, S.K., 2003. Present-day views on the environment-forming and ecological role of the Black Sea methane gas seeps. Mar. Ecol. J. 2, 5–26 (in Russian).

Finetti, I., Bricchi, G., Den Ben, A., Pipan, M., Huan, Z., 1988. Geophysical study of the Black Sea. Boll. Geofis. Teor. Appl. (Monografia Black Sea) XXX (117–118), 197–324.

Heeschen, K.U., Tréhu, A.M., Collier, R.W., Suess, E., Rehder, G., 2003. Distribution and height of methane bubble plumes on the Cascadia Margin characterized by acoustic imaging. Geophys. Res. Lett. 30, 1643, doi:10.1029/2003GL016974.

Ivanov, M.K., Limonov, A.F., van Weering, T.C.E., 1996. Comparative characteristics of the Black Sea and Mediterranean mud volcanoes. Mar. Geol. 132, 253–271.

Johnson, J.E., Goldfinger, C., Suess, E., 2003. Geophysical constraints on the surface distribution of authigenic carbonates across the Hydrate Ridge region, Cascadia Margin. Mar. Geol. 202, 79–120.

Klaucke, I., Sahling, H., Bürk, D., Weinrebe, W., Bohrmann, G., 2005. Mapping deep-water gas emissions with sidescan sonar. EOS 86, 341–346.

Krastel, S., Spiess, V., Ivanov, M.K., Weinrebe, W., Bohrmann, G., Shashkin, P., Heidersdorf, F., 2003. Acoustic investigations of mud volcanoes in the Sorokin Trough, Black Sea. Geo-Mar. Lett. 23, 230–238.

Le Bas, T.P., Mason, D.C., Millard, N.W., 1995. TOBI image processing—the state of the art. IEEE J. Oceanic Eng. 20, 85–93.

Leifer, I., MacDonald, I., 2003. Dynamics of the gas flux from shallow gas hydrate deposits; interaction between oily hydrate bubbles and the oceanic environment. Earth Planet. Sci. Lett. 210, 411–424.

Limonov, A.F., Ivanov, M.K., Woodside, J. (Eds.), 1994. Mud volcanism in the Mediterranean and Black Sea and shallow structure of the Erastostene seamount: initial results of the geological and geophysical investigations during the 3rd UNESCO-ESF "Training-Trough-Research" cruise of RV Gelenzhik. UNESCO Reports in Marine Science, vol. 64. 173 pp.

Limonov, A.F., van Weering, T.C.E., Kenyon, N.H., Ivanov, M.K., Meisner, L.B., 1997. Seabed morphology and gas venting in the Black Sea mud volcano area: observations with the MAK-1 deep-tow sidescan sonar and bottom profiler. Mar. Geol. 137, 121–136.

Luff, R., Greinert, J., Wallmann, K., Klaucke, I., Suess, E., 2005. Simulation of long-term feedbacks from authigenic carbonate crust formation at cold vent sites. Chem. Geol. 216, 157–174.

MacDonald, I.R., Buthman, D.B., Sager, W.W., Peccini, M.B., Guinasso Jr., N.L., 2000. Pulsed flow from a Gulf of Mexico mud volcano. Geology 28, 907–910.

Mazzini, A., Ivanov, M.K., Parnell, J., Stadnitskaia, A., Cronin, B.T., Poludetkina, E., Mazurenko, L.L., van Weering, T.C.E., 2004. Methane-related authigenic carbonates from the Black Sea: geochemical characterisation and relation to seeping fluids. Mar. Geol. 212, 153–181.

Michaelis, W., Seifert, R., Nauhaus, K., Treude, T., Thiel, V., Blumenberg, M., Knittel, K., Gieseke, A., Peterknecht, K., Pape, T., Boetius, A., Amann, R., Jørgensen, B.B., Widdel, F., Peckmann, J., Pimenov, N.V., Gulin, M.B., 2002. Microbial reefs in the Black Sea fuelled by anaerobic oxidation of methane. Science 297, 1013–1015.

Milkov, A.V., Dickens, G.R., Claypool, G.E., Lee, Y.-J., Borowski, W. S., Torres, M.E., Xu, W., Tomaru, H., Tréhu, A.M., Schultheiss, P., 2004. Co-existence of gas hydrate, free gas and brine within the regional gas hydrate stability zone at the Southern Summit of Hydrate Ridge (Oregon Margin): evidence from prolonged degassing of a pressurized core. Earth Planet. Sci. Lett. 222, 829–843.

Naudts, L., Greinert, J., Artemov, Y., Staelens, P., Poort, J., Van Rensbergen, P., De Batist, M., 2006. Geological and morphological setting of 2778 methane seeps in the Dnepr paleo-delta, northwestern Black Sea. Mar. Geol. 227, 177–199.

Neretin, L., Böttcher, M.E., Jørgensen, B.B., Volkov, I.I., Lüschen, H., Hilgenfeldt, K., 2004. Pyritization processes and greigite formation in the advancing sulfidization front in the Upper Pleistocene sediments of the Black Sea. Geochim. Cosmochim. Acta 68, 2081–2093.

Nikishin, A.M., Korotaev, M.V., Ershov, A.V., Brunet, M.-F., 2003. The Black Sea basin: tectonic history and Neogene–Quaternary rapid subsidence modelling. Sediment. Geol. 156, 149–168.

Rangin, C., Bader, A.G., Pascal, G., Ecevitoğlu, B., Görür, N., 2002. Deep structure of the Mid Black Sea High (offshore Turkey) imaged by multi-channel seismic survey (BLACKSIS cruise). Mar. Geol. 182, 265–278.

Reeburgh, W.S., Ward, B.S., Whalen, S.C., Sandbeck, K.A., Kilpatrick, K.A., Kerkhof, L.J., 1991. Black Sea methane geochemistry. Deep-Sea Res. 38, S1189–S1210.

Robinson, A.G., Griffith, E.T., Gardiner, A.R., Home, A.K., 1997. Petroleum geology of the Georgian fold and thrust belts and foreland basins. In: Robinson, A.G. (Ed.), Regional and Petroleum Geology of the Black Sea and Surrounding Region. APG Memoir, vol. 68. AAPG, Tulsa, pp. 347–367.

Ross, D.A., Degens, E.T., 1974. Recent sediments of the Black Sea. In: Degens, E.T., Ross, D.A. (Eds.), The Black Sea—Geology, Chemistry and Biology. AAPG Memoir, vol. 20. AAPG, Tulsa, pp. 183–199.

Ruppel, C., Dickens, G.R., Castellini, D.G., Gilhooly, W., Lizarralde, D., 2005. Heat and salt inhibition of gas hydrate formation in the northern Gulf of Mexico. Geophys. Res. Lett. 32, doi:10.1029/2004GL021909.

Rusanov, I.I., Pimenov, N.V., Yusupov, S.K., Savichev, A.S., Ivanov, M.V., 2005. Microbial production and transformation of methane in the deep sea zone of the Black Sea. International workshop on "Methane in sediments and water column of the Black sea: Formation, transport pathways and the role within the carbon cycle", Sevastopol, Ukraine, May 17–22, 2005.

Sager, W.W., MacDonald, I.R., Hou, R., 2004. Sidescan sonar imaging of hydrocarbon seeps on the Louisiana continental slope. AAPG Bull. 88, 725–746.

Sahling, H., Blinova, V., Bürk, D., Çifçi, G., Çopur, S., Dondurur, D., Klaucke, I., Lursmanashvili, N., Okay, S., Renken, J., Schott, T., 2004. Report and preliminary results of R/V Poseidon cruise P317/4 Istanbul–Istanbul 16 October–4 November 2004. Berichte FB Geowiss., vol. 235. Universität Bremen. 92 pp.

Sassen, R., Roberts, H.H., Carney, R., Milkov, A.V., DeFreitas, D.A., Lanoil, B., Zhang, C., 2004. Free hydrocarbon gas, gas hydrate, and authigenic minerals in chemosynthetic communities of the northern Gulf of Mexico continental slope: relation to microbial processes. Chem. Geol. 205, 195–217.

Schmale, O., Greinert, J., Rehder, G., 2005. Methane emissions from high-intensity marine gas seeps in the Black Sea into the atmosphere. Geophys. Res. Lett. 32, L07609, doi:10.1029/2004GL021138.

Shoji, H., Soloviev, V., Matveeva, T., Mazurenko, L.L., Minami, H., Hachikubo, A., Sakagami, H., Hyakutake, K., Kaulio, V., Gladysch, V., Logvina, E., Obzhirov, A., Baranov, B., Khlystov, O., Biebow, N., Poort, J., Jin, Y.K., Kim, Y., 2005. Hydrate-bearing structures in the Sea of Okhotsk. EOS 86, 13–18.

Sloan, E.D., 1990. Clathrates Hydrates of Natural Gases. Marcel Dekker Publishing, New York. 641 pp.

Suess, E., Torres, M.E., Bohrmann, G., Collier, R.W., Greinert, J., Linke, L., Rehder, G., Trehu, A., Wallmann, K., Winckler, G., Zuleger, E., 1999. Gas hydrate destabilization: enhanced dewatering, benthic material turnover and large methane plumes at the Cascadia convergent margin. Earth Planet. Sci. Lett. 170, 1–15.

Stoll, R.D., 1986. Acoustic waves in marine sediments. In: Akal, T., Berkson, J.M. (Eds.), Ocean Seismo-acoustics; Low-frequency Underwater Acoustics. Plenum Press, New York, pp. 417–434.

Tréhu, A.M., Long, P.E., Torres, M.E., Bohrmann, G., ODP Leg 204 Shipboard Party, 2004. Three-dimensional distribution of gas hydrate beneath southern Hydrate Ridge: constraints from ODP Leg 204. Earth Planet. Sci. Lett. 222, 845–862.

Torres, M.E., McManus, J., Hammond, D.E., de Angelis, M.A., Heeschen, K.U., Colbert, S.L., Tryon, M.D., Brown, K.M., Suess, E., 2002. Fluid and chemical fluxes in and out of sediments hosting methane hydrate deposits on Hydrate Ridge, OR: I. Hydrological provinces. Earth Planet. Sci. Lett. 201, 525–540.

Tugolesov, D.A., Gorshkov, A.S., Meisner, L.B., Soloviev, V.V., 1985. Tectonics of the Mesozoic–Cenozoic Deposits of the Black Sea Basin. Nedra, Moscow. 215 pp. (in Russian).

Zonenshain, L.P., Le Pichon, X., 1986. Deep basins of the Black Sea and Caspian Sea as remnants of Mesozoic back-arc basins. Tectonophysics 123, 181–211.